Heliyon 10 (2024) e23686

Contents lists available at ScienceDirect

Heliyon

journal homepage: www.cell.com/heliyon

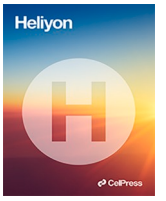

Prognostic and metabolic characteristics of a novel cuproptosis-related signature in patients with hepatocellular carcinoma

Xin Qu [a,1], Ling-cui Meng [a,1], Xi Lu [b], Xian Chen [c], Yong Li [a], Rui Zhou [a], Yan-juan Zhu [d], Yi-chang Luo [a], Jin-tao Huang [e], Xiao-liang Shi [f], Hai-Bo Zhang [f,*]

[a] *Department of Oncology, The Second Affiliated Hospital of Guangzhou University of Chinese Medicine, Guangdong Provincial Hospital of Traditional Chinese Medicine, Guangzhou, 510120, China*
[b] *Department of Ultrasound, The Second Affiliated Hospital of Guangzhou University of Chinese Medicine, Guangdong Provincial Hospital of Traditional Chinese Medicine, Guangzhou, 510120, China*
[c] *Guangzhou Hospital of Traditional Chinese Medicine Affiliated to Guangzhou University of Traditional Chinese Medicine, Guangzhou, 510405, China*
[d] *The Second Clinical Medical School of Guangzhou University of Chinese Medicine, Guangzhou, 510120, China*
[e] *Department of Oncology, Guangzhou Hospital of Traditional Chinese Medicine Affiliated to Guangzhou University of Traditional Chinese Medicine, Hospital of Traditional Chinese Medicine Affiliated to Guangzhou Medical University, Guangzhou, 510130, China*
[f] *Shanghai OrigiMed Co., Ltd, Shanghai, 201114, China*

ARTICLE INFO

Keywords:
Cuproptosis
HCC
Metabolism
Prognosis
Treatment

ABSTRACT

Cuproptosis is a novel discovered mode of programmed cell death. To identify the molecular regulatory patterns related to cuproptosis, this study was designed for exploring the correlation between cuproptosis-related genes (CRGs) and the prognosis, metabolism, and treatment of hepatocellular carcinoma (HCC). Cancer Genome Atlas (TCGA) database was used to screen 363 HCC samples, which were categorized into 2 clusters based on the expression of CRGs. Survival analysis demonstrated that overall survival (OS) was better in Cluster 1 than Cluster 2 which might to be relevant to differences in metabolic based on functional analysis. With LASSO regression analysis and univariate COX regression, 8 prognosis-related genes were screened, a differently expressed genes (DEGs) were then constructed (HCC patients' DEGs)-based signature. The signature's stability was also validated in the 2 independent cohorts and test cohorts (GSE14520, HCC dataset in PCAWG). The 1-year, 3-year, and 5-year area under the curve (AUC) were 0.756, 0.706, and 0.722, respectively. The signature could also well predict the response to chemotherapy, targeted and transcatheter arterial chemoembolization (TACE) by providing a risk score. Moreover, the correlation was uncovered by the research between the metabolism and risk score. In conclusion, a unique cuproptosis-related signature that be capable of predicting patients' prognosis with HCC, and offered valuable insights into chemotherapy, TACE and targeted therapies for these patients has been developed.

* Corresponding author. Department of Oncology, Guangdong Provincial Hospital of Traditional Chinese Medicine, No. 111, Dade Road, Guangzhou, Guangdong, 510120, China.
E-mail address: haibozh@gzucm.edu.cn (H.-B. Zhang).
[1] Xin Qu and Ling-cui Meng contributed equally to this work as co-first authors.

https://doi.org/10.1016/j.heliyon.2023.e23686
Received 26 March 2023; Received in revised form 29 November 2023; Accepted 9 December 2023
Available online 29 December 2023

1. Impact statement

This study aimed to analyze the relationship between hepatocellular carcinoma and cuproptosis-related genes. We developed a risk score that could be the prognostic predictor in patients with HCC, as well as the sensitivity to chemotherapy, targeted and transcatheter arterial chemoembolization. Simultaneously, we also found that the two diametrically opposed prognostic outcomes also differ significantly in metabolic features. Therefore, we hypothesized that distinct patterns of cuproptosis may impact prognoses of HCC patients, which is likely to be associated with metabolic features.

2. Introduction

Hepatocellular carcinoma (HCC) occupied approximately 75%–85 % of primary liver cancer, which was the worldwide 6th most prevalent cancer globally and was the 3rd leading cause of cancer-related mortality in 2020 [1]. Currently, the preferred clinical treatment for liver cancer is radical surgery at early stages. However, because there is no obvious symptom at the early stages, most patients are not diagnosed until the middle-to-late stages, hence, only a minority of patients benefit from restricted treatment. Therefore, it's critical to recognize neoteric biomarkers for predicting prognosis and guiding the therapy.

In March 2022, "cuproptosis" was first proposed as a novel cell death mode similar to ferroptosis [2], which is characterized by inducing fatty acylated proteins through directly binding to the fatty acylated moiety of the tricarboxylic acid cycle. The aggregation and destabilization of iron-sulfur cluster protein may lead to proteotoxic stress inducing apoptosis-independent cell death [3]. Previous studies have identified 10 cuproptosis-related genes (CRGs) including *FDX1*, *LIPT1*, *DLD*, *LIAS*, *PDHA1, DLAT*, *PDHB*, *MTF1*, *GLS*, and

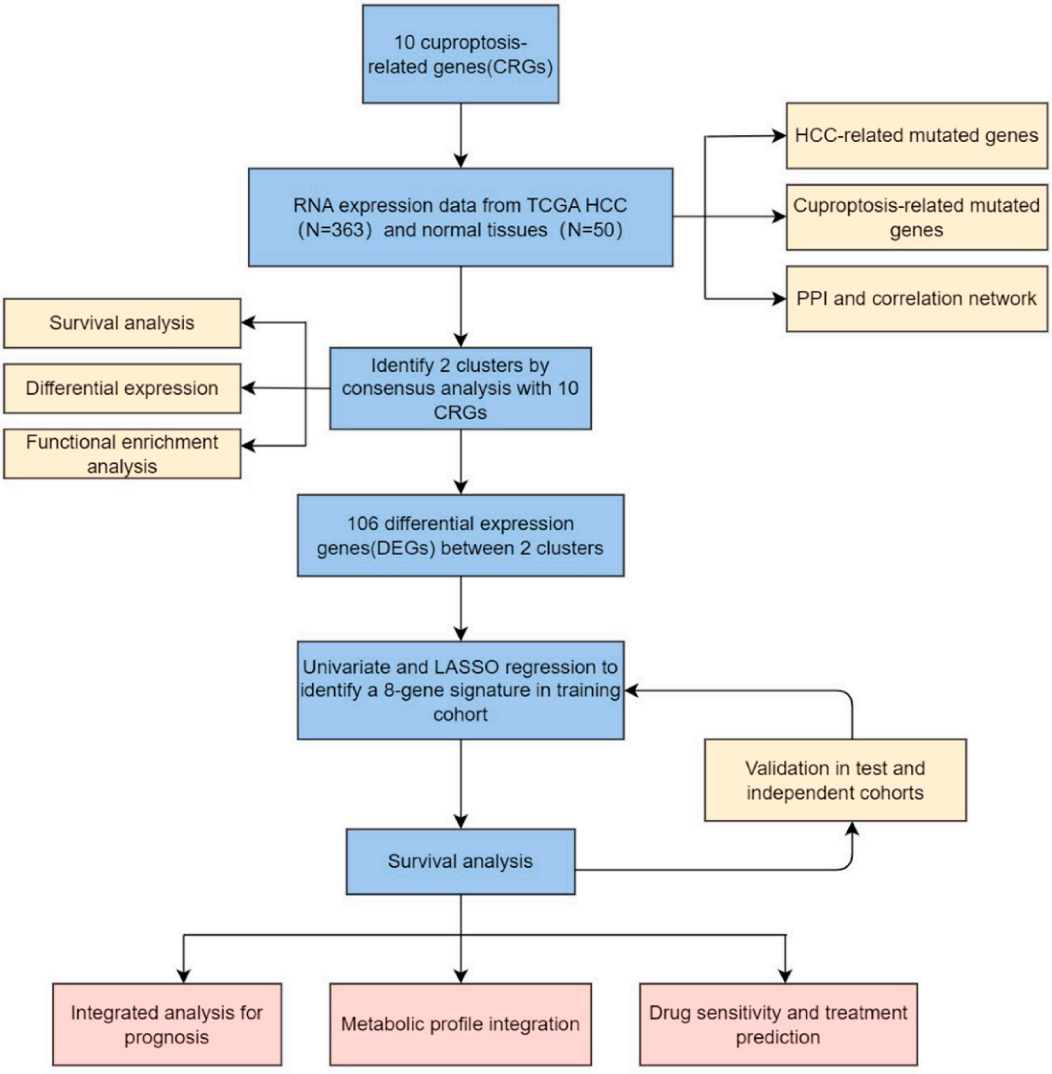

Fig. 1. Workflow diagram. A diagram illustrating the primary stages involved in this study.

CDKN2A [3]. All these genes were closely related to metabolic pathways. For example, *FDX1* is a key factor in regulating cuproptosis and has been proven to be involved in glucose metabolism, fatty acid oxidation, and amino acid metabolism [4]; *LIAS*, *LIPL1,* and *DLD* are also associated with protein lipid acylation metabolism; and *DLAT*, *PDHA*1, *PDHB*, *MTF1*, *GLS*, and *CDKN2A* are related to forming of pyruvate dehydrogenase complex [3].

Copper is the third most basic trace metal in living organisms, which is involved in mitochondrial energy production, antioxidant defense, and other functions. When there is an excess of copper in cells or when its distribution within cells is inadequate, it can lead to the occurrence of copper-dependent cytotoxicity. This phenomenon is associated with the development of diseases and has a strong correlation with various types of cancer [5]. Research has indicated that the presence of copper in tissues can potentially enhance the production of nitric oxide and mediators, thereby potentially triggering the initiation of pro-angiogenic signaling within tumors [6]. A variety of cancer tissues exhibit increased levels or systemic distribution of copper ions, such as breast cancer [7] and cervical cancer [8]. However, research is currently being conducted to elucidate the relationship between cuproptosis and HCC.

The study was to dissect the association between CRGs and HCC. We devised a risk score capable of forecasting the prognosis of HCC patients, as well as their responsiveness to chemotherapy, targeted therapies, and transcatheter arterial chemoembolization (TACE).

3. Materials and methods

A visual representation illustrating the sequence of steps undertaken in this study can be observed in Fig. 1.

3.1. Datasets and preprocessing

Information on 371 HCC patients was extracted from The Cancer Genome Atlas (TCGA) database (371 patients have the genomic and clinical information, and 363 patients have transcriptomic data). The GEO database was utilized to obtain three datasets (GSE14520, GSE109211, GSE104580) related to HCC, and one was obtained from the PCAWG (Pan-Cancer Analysis of Whole Genomes) database.

3.2. Mutations, expression, and interactions of CRGs

The Maftools package was utilized to visualize the genetic landscape of HCC. The Wilcox test was employed to evaluate the disparity in expression levels of the 10 CRGs between HCC and adjacent non-cancerous tissues. The Search Tool for the Retrieval of Interaction Genes (STRING version 11.0) was developed to make the protein-protein interaction (PPI) network [9]. R package was used in these procedures, including ggplot2 (version 3.3.5), reshape (version 0.8.8), and igraph (version 1.2.7) [10].

3.3. Unsupervised clustering

Utilizing K-means analysis, a total of 363 samples were categorized into two entirely distinct clusters in terms of the expression patterns of 10 CRGs. To ensure reliable classification, this process was iterated 1000 times to achieve consistent results [11]. A consensus algorithm was subsequently employed to modify the quantities of clusters.

3.4. Detection of genes with distinct expression patterns (DEGs) and functional characterization

Using the limma package, 106 differently expressed genes were identified in 2 clusters according to the criteria of $|\log FC| > 1$ and p-adjust <0.05 (The correction method was Benjamini & Hochberg method). Metascape was performed for pathway enrichment and biological process annotation of DEGs. GSEA was used to discover how these two clusters were associated with specific biological significance from an expression perspective.

3.5. Construction of cuproptosis-related prognostic signature

By conducting an analysis on 106 DEGs, we employed a random allocation method to divide the total of 363 samples into 2 separate groups of training group and test group. The ratio between these groups was set at 7:3. In the training cohort, univariate COX regression analysis was initially performed to ascertain genes associated with prognosis. Next, we employed LASSO regression to identify potential markers and establish a prognostic signature specifically associated with cuproptosis. We categorized the samples into 2 groups, namely low- and high-risks, depending on the risk score that falls within the median range. To assess the survival outcomes, we performed a Kaplan-Meier analysis to compare the two groups. Time-dependent receiver operating characteristic (ROC) curves were employed to evaluate the predictive efficiency of the signature, which was subsequently validated using both a test dataset and two additional independent datasets.

3.6. Drug sensitivity assessment and treatment prediction

The sensitivity of each sample from TCGA to cisplatin and gemcitabine was predicted using the pRRophetic package, and the drug IC50 values were evaluated according to the signature. In addition, associations between the signature with TACE and sorafenib

treatment response were evaluated based on GSE109211 and GSE104580 datasets.

3.7. Correlation between risk scores and metabolism

For assessing the associaion between cuproptosis and individual metabolic pathways, metabolism-related genes were compiled from the Molecular Signatures Database (MSigDB) and pathway scores was determined using ssGSEA. The relationship between the risk score and various metabolic pathways was examined through Spearman correlation analysis. To visualize these correlations, R software packages such as "corrplot", "ggpubr", and "ggplot2" was utilized.

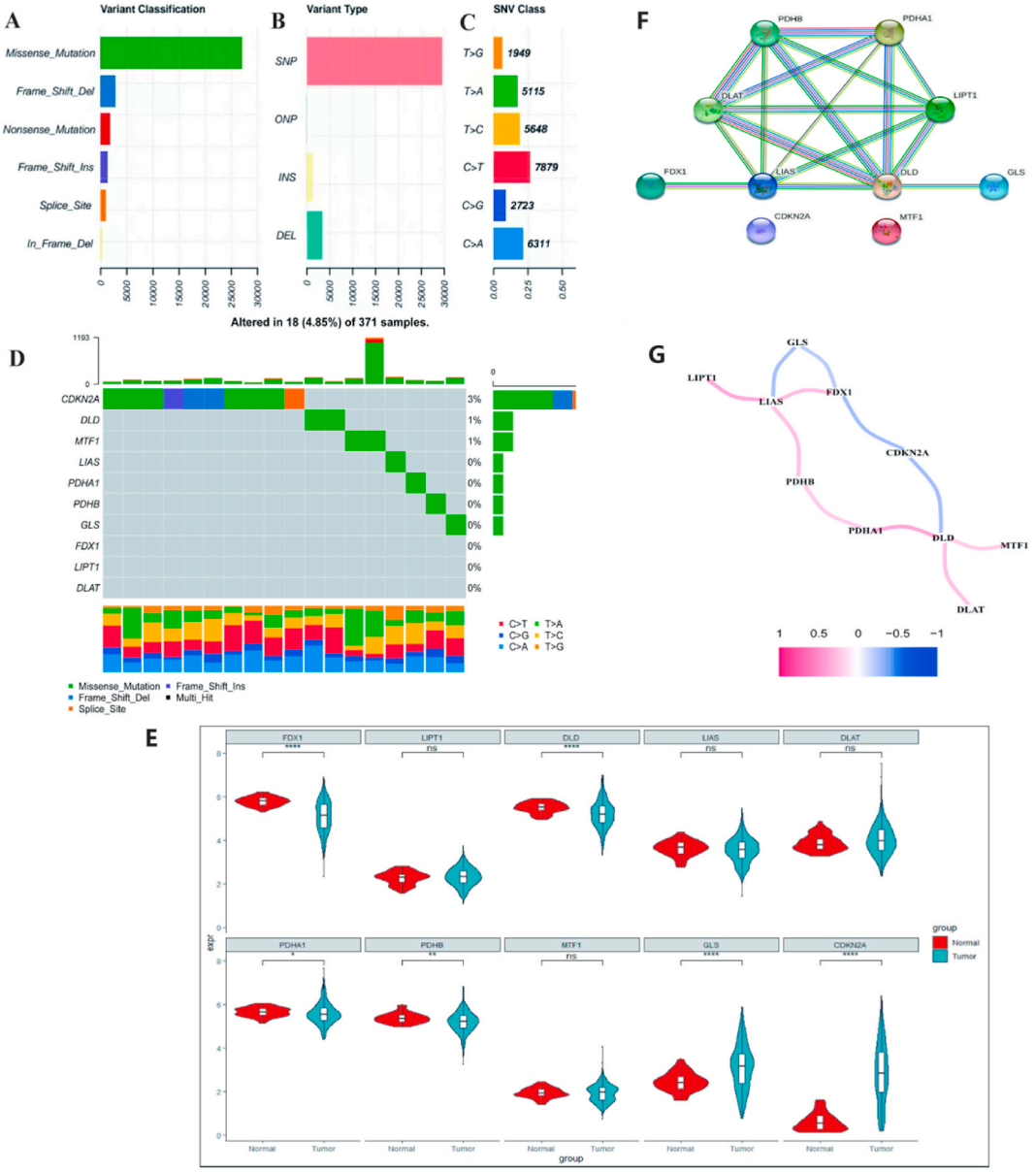

Fig. 2. Genetic and expression profiles of genes associated with cuproptosis in individuals diagnosed with HCC. (A)–(C) Based on mutant frequency, type, and classification of 371 TCGA samples. (D) Waterfall plot revealed 18 of the 371 samples (4.85 %) showed mutations associated with cuproptosis. (E) The hepatic expression of ten genes associated with cuproptosis in cases of HCC and paracancer. Cyan color: tumor samples; red color: paracancer samples. Statistical variances are indicated by asterisks, with varying numbers of asterisks representing different degrees of significance. (F) The network of PPI of genes associated with cuproptosis. (G) The network of CRGs exhibits positive correlation hinted by red color, negative correlation implied by blue, and no correlation denoted as 0.

3.8. Statistical analysis

Difference analysis of continuous data was analyzed by the Shapiro-Wilk test, and the Chi-squared Test adopted Levene's test. Spearman's rank correlation method was applied for calculating correlation coefficients. Data identical with a standard normal distribution and uniform variance were tested using two-sample *t*-test, otherwise the Wilcox test was used. Log-rank test was used for survival analysis. Differences in *P* value less than 0.05 were considered statistically significant: $^{*}P < 0.05$, $^{**}P < 0.01$, $^{***}P < 0.001$, $^{****}P < 0.0001$.

4. Results

4.1. Mutation characteristics and expression pattern of CRGs in HCC patients

In regarding to the mutations among HCC patients, the commonest variant type was missense mutation of CRGs, and single nucleotide polymorphism (SNP) was the predominant variation type, mainly manifested as C > T mutation (Fig. 2A–C). CRGs mutation was observed in 18 out of 371 samples (4.85 %) (Fig. 2D). Among them, the most frequent mutated gene was *CDKN2A* (3 %), followed by *DLD* (1 %) and *MTF1* (1 %). No mutations were detected in *FDX1*, *LIPT1*, and *DLAT*. Compared to paracancerous tissues, up-

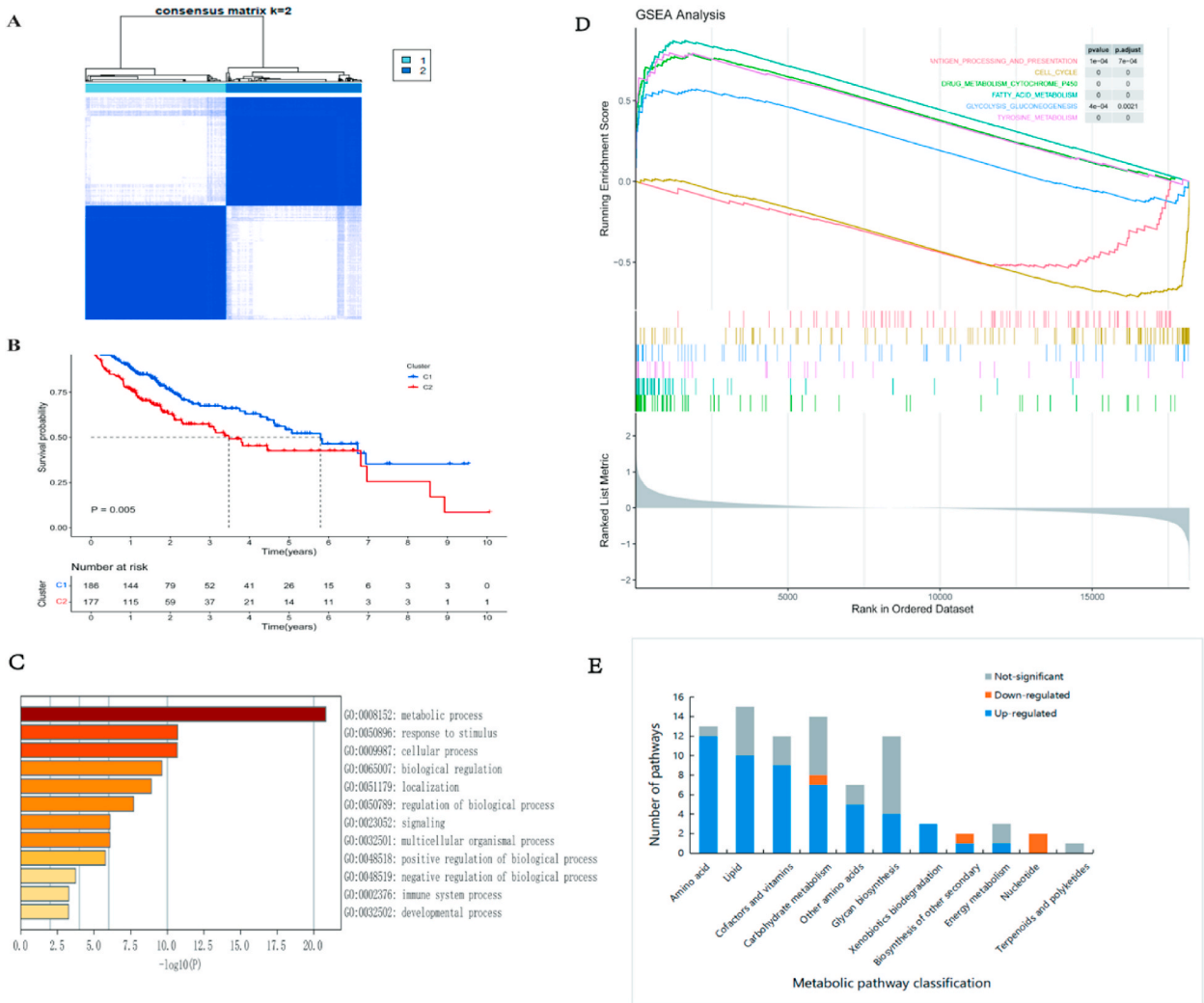

Fig. 3. Identification of cuproptosis-related subtypes. **(A)** The training set exhibits a consensus matrix that demonstrates optimal inter-group correlation at $k = 2$, while minimizing inter-group correlation **(B)** Relevant clusters associated with cuproptosis exhibited distinct OS curves(log-rank test, $P = 0.005$). **(C)** Colored bar charts displaying enriched terms for genes that exhibit differential expression between two clusters related to cuproptosis, with significance levels indicated by *p*-value. **(D)** Gene sets exhibiting enrichment in KEGG. The left denotes Cluster 1, while the right corresponds to Cluster 2 **(E)** The horizontal and ordinate coordinates represent the number of expressions and the name of metabolic pathway, respectively. Grey, orange and blue represent not-significant, down-regulated, up-regulated, respectively.

regulated expression of *DLAT*, *GLS*, *CDKN2A*, and *MTF1* but down-regulated expression of *FDX1*, *DLD*, and *LIAS* were observed in tumor tissues (Fig. 2E). A PPI analysis was further performed to investigate the interaction of CRGs (Fig. 2F). The co-expression network analysis displayed a positive association between the expression of *FDX1* and *LIAS*, while it exhibited a negative correlation with *GLS* and *CDKN2A* expressions. Additionally, *LIAS* expression was negatively associated with *GLS* but positively related to *LIPT1* and *PDHB* expressions. The correlations of other CRGs can be observed in Fig. 2G.

4.2. Identification of cuproptosis-related clusters

Based on the transcriptional level of 10 CRGs, K-means analysis was used for clustering 363 samples into 2 different molecular patterns (Fig. 3A, Supplementary Figures S1 and S2), consisting of 341 samples, with Cluster 1 containing 178 samples and 163 in Cluster 2. Cluster 1 was characterized as significant upregulation of *FDX1*, *DLD*, and *LIAS*, and significant downregulation of *DLAT*, *GLS*, and *CDKN2A* (Supplementary Figure S3). Survival analysis showed that Cluster 1 had better OS ($P = 0.005$, Fig. 3B). We identified 106 DEGs which mainly enriched in metabolic pathways between the two clusters (Supplementary Table S2). Functional annotation by Metascape software validated that DEGs were mainly enriched in metabolic pathways (Fig. 3C). In GSEA analysis of cluster 1, pathways of antigen processing and presentation, cell cycle were downregulated; pathways of drug metabolism cytochrome p450, fatty acid metabolism, tyrosine metabolism, and glycolysis/glycogen were upregulated. (Fig. 3D). Furthermore, the analysis of KEGG (Kyoto Encyclopedia of Genes and Genomes) demonstrated that most pathways, such as amino acid metabolism, lipid metabolism, cofactor and vitamin metabolism, carbohydrate metabolism were upregulated in Cluster 1, however, genes associated with nucleotide metabolism pathway were significantly downregulated (Fig. 3E).

4.3. Construction and validation of cuproptosis-related risk scores

DEGs-based prognostic signature was generated to analyze the underlying relationship between CRGs and prognosis. The method involved randomly assigning 363 patients into training group (254 patients) and test group (109 patients) with the ratio of 7:3. Subsequently, the training set was utilized to identify 74 genes in correlation to prognosis in univariate COX model. These potential markers were furtherly narrowed down by LASSO regression to determine a cuproptosis-related signature that showed a significant association with prognosis (Supplementary Figures S4 and S5). The risk score was calculated as follows:

Risk score = (−0.002**CYP2C9*) + (−0.011**FTCD*) + (−0.043**CPS11*) + (0.054**SPP1*) + (−0.029**SLC17A2*) + (0.021**G6PD*) + (−0.072**DNASE1L3*) + (0.101**CDCA8*) (Table 1)

In the training group, a classification was performed on the 254 patients into high- and low-risk groups using the medians for survival analysis. The consequence indicated that lower OS was linked with higher risk scores ($P < 0.001$, Fig. 4A). The outcomes of principal component analysis could be observed in Fig. 4C and F. The ROC curves, which vary with time, and the AUC values at 1, 3, and 5 years were 0.756, 0.706, and 0.722 respectively (Fig. 4B). The outcome was verified in the test cohorts and the 2 independent validation cohorts (Fig. 4D–E, Fig. 5A–B). Univariate and multivariate regression models were utilized to estimate the risk score of cuproptosis-related signature adjusting for relevant clinical variables, including age, sex, cell type and stage, body mass index, and platelet count. Univariate analysis demonstrated a significant association between higher risk scores and a worse prognosis ($P < 0.001$, HR: 3.701,95 % CI: 2.533–5.405, Fig. 6A). Multifactorial analysis displayed that the risk score was an independent prognostic factor in HCC patients ($P < 0.001$, HR: 2.586,95 % CI: 1.530–4.373, Fig. 6B). Similarly, the ROC curves proved the risk score had a more significant advantage than other clinical parameters. Additionally, previous literature reported some HCC-related prognostic signature [12–17], among which ZYQ et al. reported the highest AUC value for signature [15]. However, the result showed that the signature in this research had better predictive ability than ZYQ et al.'s (Fig. 7).

4.4. The role of risk scores in drug sensitivity and prediction of treatment

We further evaluated the sensitivity of cisplatin and gemcitabine, two chemotherapeutic agents frequently employed, in patients exhibiting varying risk scores associated with CRGs. The findings indicated that cisplatin and gemcitabine exhibited higher efficacy in

Table 1
Cuproptosis-related signature score and coefficients.

Gene symbol	Description	Coefficient
CYP2C9	Cytochrome P450 Family 2 Subfamily C Member 9	−0.00249604340873695
FTCD	Formiminotransferase Cyclodeaminase	−0.0115596836384986
CPS1	Carbamoyl-Phosphate Synthase 1	−0.043767603273062
SPP1	Secreted Phosphoprotein 1	0.0543191185045022
SLC17A2	Solute Carrier Family 17 Member 2	−0.0294564227749715
G6PD	Glucose-6-Phosphate Dehydrogenase	0.0215855311755536
DNASE1L3	Deoxyribonuclease 1 Like 3	−0.0724899606045817
CDCA8	Cell Division Cycle Associated 8	0.101730840983151

*HCC, hepatocellular carcinoma; CRGs, cuproptosis-associated genes; PPI, protein-protein interaction; OS, overall survival; ROC, receiver operating characteristic; PCA, principal component analysis; TACE, transcatheter arterial chemoembolization; KEGG, Kyoto Encyclopedia of Genes and Genomes.

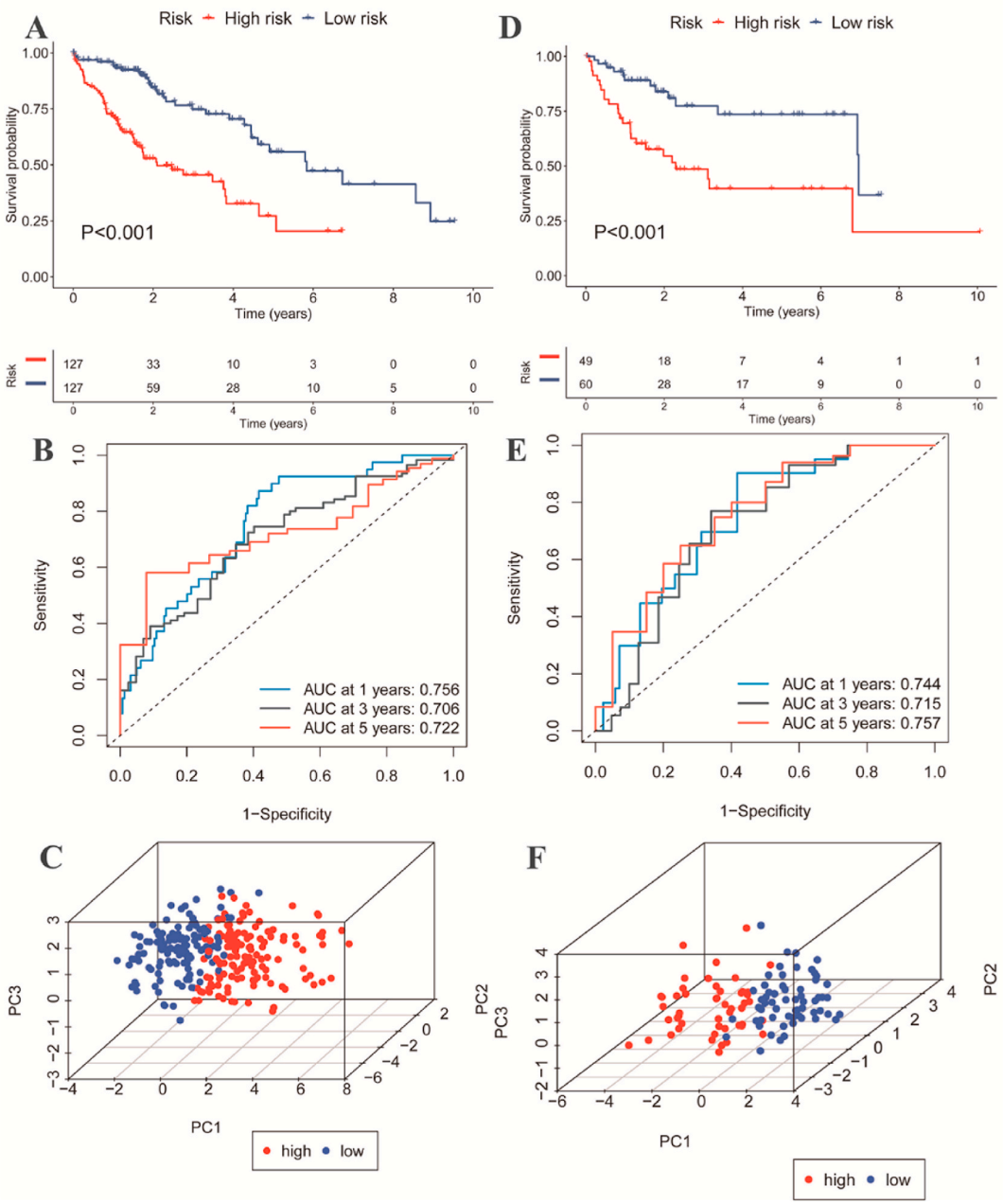

Fig. 4. Development and verification of the signature associated with cuproptosis. (A) Kaplan-Meier curves were generated to assess OS in the training set, based on risk groups associated with cuproptosis. The statistical significance was determined using a log-rank test. **(B)** ROC curve of the risk score for the training set. **(C)** The risk group-related PCA analysis pertains to cuproptosis. **(D–F)** Kaplan-Meier and ROC curves and PCA analysis of cuproptosis-related risk groups in the test set.

treating patients classified as low-risk compared to those categorized as high-risk group ($P < 0.0001$ and $P < 0.05$, respectively) (Fig. 8A and B).

Sorafenib is presently regarded as the primary targeted medication for the systemic management of individuals diagnosed with advanced HCC [18]. Additionally, TACE is suggested as a viable treatment alternative for advanced liver carcinoma in international guidelines addressing the management of inoperable hepatic malignancies [19]. Therefore, further investigation of the associations between response to sorafenib, TACE and risk score found that patients who responded to sorafenib and TACE exhibited significantly higher risk scores compared to the non-responders ($P < 0.01$ and $P < 0.0001$, respectively; Fig. 8C and D).

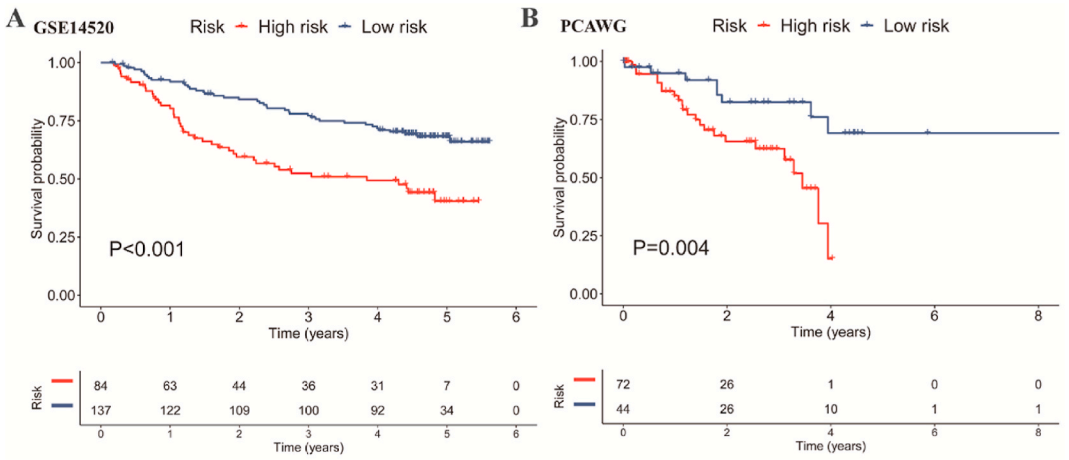

Fig. 5. External verification of the cuproptosis-related signature. (A–B) External verification of signature based on two independent sets (GSE14520, PCAWG).

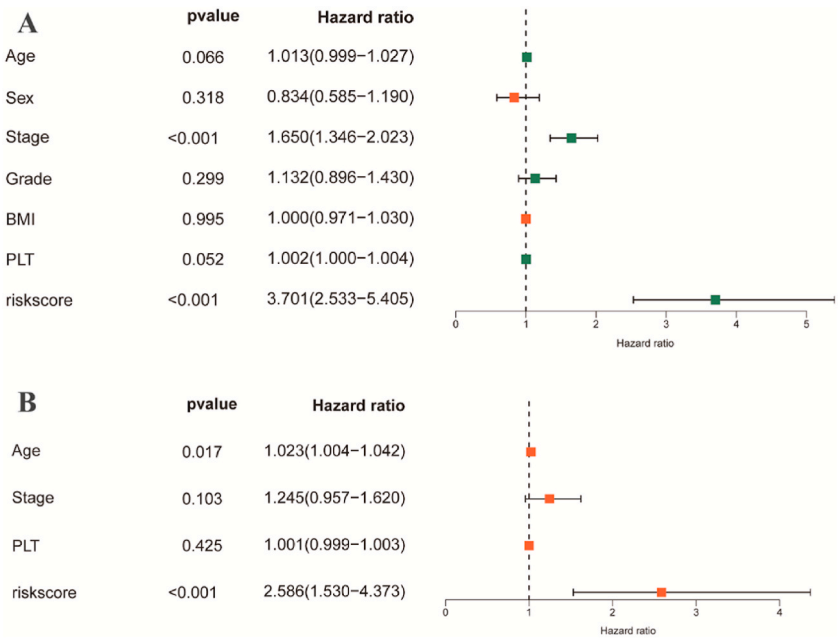

Fig. 6. Cox regression analysis of risk scores. (A–B) Univariate and multivariate Cox regression of OS in the TCGA cohort.

4.5. Risk score is associated with metabolic pathways

Additionally investigation into the correlation between the metabolism-related pathways and risk score revealed significant correlations. Specifically, the risk score was observed to be a detrimental correlation with Glycine, serine, and threonine metabolism (R = 0.46, $P < 2.2e\text{-}16$, Fig. 9B), as well as the Tricarboxylic acid (TCA) cycle (R = 0.64, $P < 2.2e\text{-}16$, Fig. 9A). On the other hand, it showed a positive correlation with Pyrimidine metabolism (R = 0.25, $P = 1.1e\text{-}06$, Fig. 9C) and the Pentose phosphate pathway (R = 0.31, $P = 1.4e\text{-}09$, Fig. 9D).

5. Discussion

HCC is a type of cancerous tumor that exhibits significant morbidity and mortality rates, lacking evident symptoms during its initial phases and demonstrating a relatively poor 5-year survival rate [20,21]. Cuproptosis is a newly discovered type of programmed cell death that has been proved to be closely associated with the progression of a variety of tumors [22]. It is anticipated to be target-effective for selectively inducing cell death in cancer. Hence, it is crucial to determine the responsiveness and outlook of HCC

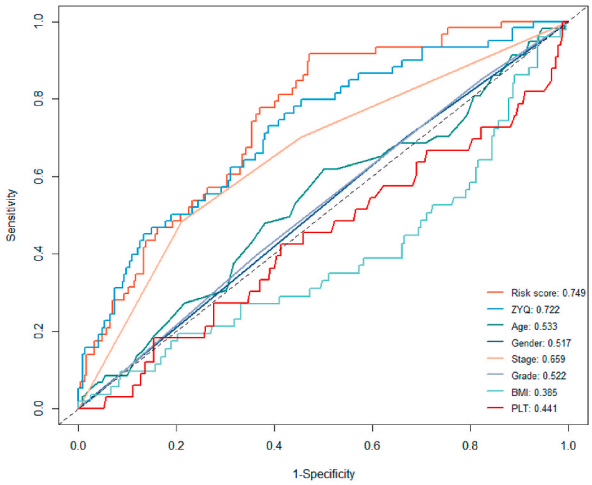

Fig. 7. The ZYQ, age, sex, pathological type and stage, body mass index, and platelet count were the respective areas under the ROC curve.

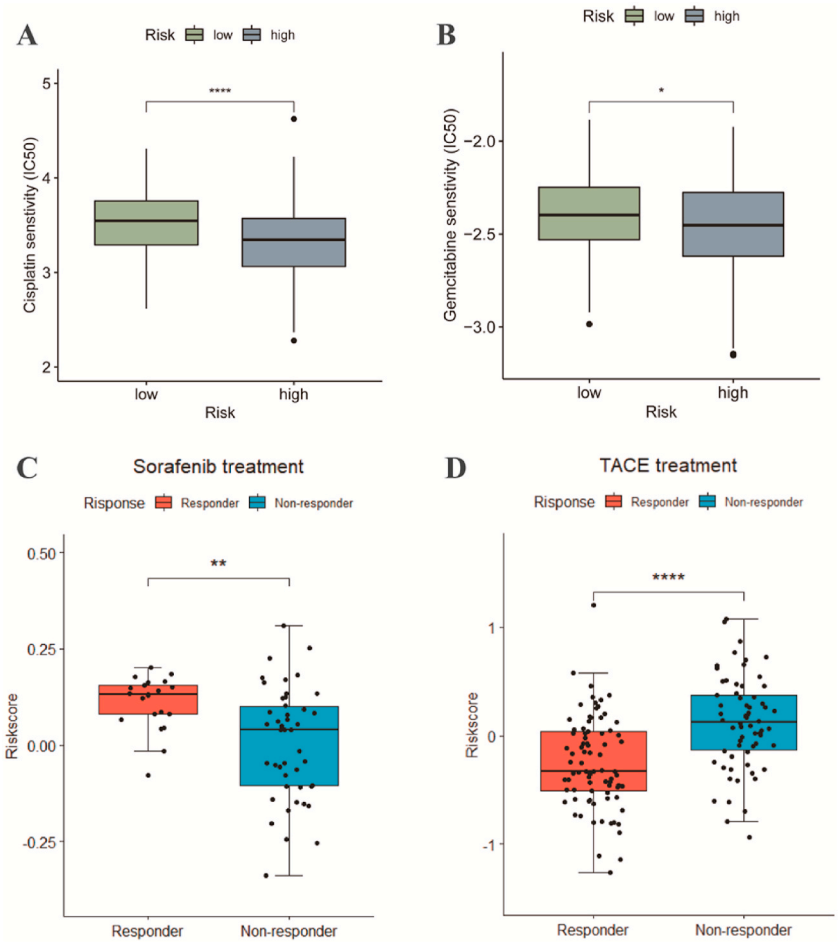

Fig. 8. Screening potential treatment for HCC. (A–B) Two medications, sorafenib and gemcitabine, exhibit significant variations in drug responsiveness among low- and high-risk populations. **(C–D)** Boxplots of risk score reactivity to sorafenib and TACE.

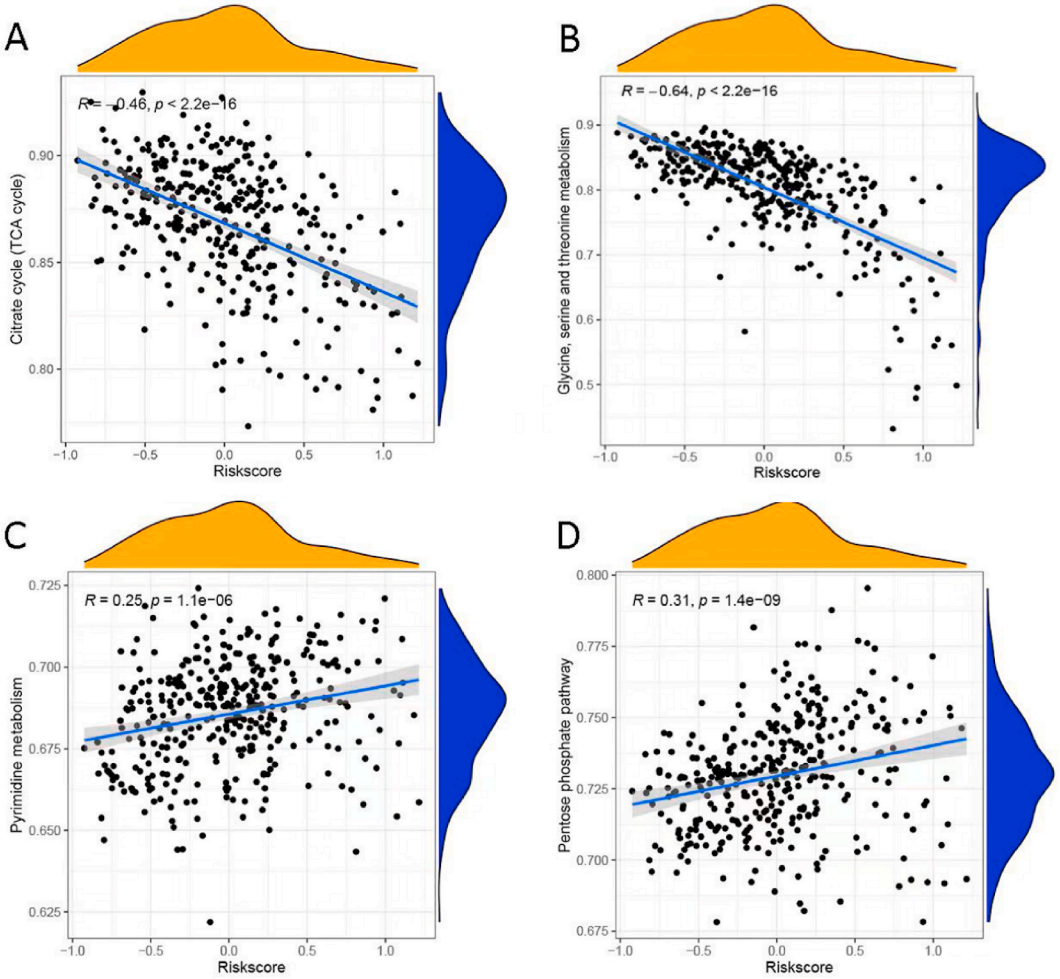

Fig. 9. The scatter diagram of correlation analysis between risk scores and metabolic pathways. (A) Citrate cycle (TCA cycle); **(B)** Glycine, serine and threonine metabolism; **(C)** Pyrimidine metabolism; **(D)** Pentose phosphate pathway.

individuals towards various therapies and investigate the molecular regulatory mechanism of cuproptosis in HCC. In this study, patients diagnosed with HCC were classified into two disparate groups based on the expression levels of 10 CRGs, which significantly influenced their prognosis. Next, the significant metabolic differences between these two clusters were elaborated and a DEGs-based prognostic signature was constructed. The signature has a strong correlation with the management of HCC, enabling the anticipation of cisplatin, gemcitabine, sorafenib, and TACE responsiveness in patients. Furthermore, patients with different risk scores showed different metabolic statuses. We hypothesized that distinct patterns of cuproptosis may result in the different prognoses of HCC patients, which is likely to be associated with metabolic features.

In the prognostic signature, protective genes such as *CYP2C9*, *FTCD*, *CPS11*, *SLC17A2*, and *DNASE1L3* was conversely linked to the risk score, whereas other genes had positive associations with the risk score. *CYP2C9* is a member of the cytochrome P450 (CYP) enzyme family, is found to be widely engaged in the metabolism of various carcinogens and drugs [23]. A previous study has found a significant downregulation of *CYP2C9* in HCC by hsa-miR-128-3p specifically targeting the 39-UTR of the *CYP2C9* to inhibit its expression [24]. *FTCD* is an enzyme with dual functionality that exhibits high expression levels in cell lines of mammals, and its expression is downregulated in HCC [25]. The latest research have confirmed that it is a key regulatory enzyme of histidine metabolism [26], and repression of HCC cell proliferation is observed upon the overexpression of FTCD [27]. *SLC17A2* is a key transcription factor involved in multiple metabolic pathways, which is only distributed in the cell membrane and cytoplasm of hepatocytes. It is reported that *SLC17A2* was appreciably downregulated in HCC patients, indicating a poor prognosis [28]. *DNASE1L3*, a member of the deoxyribonuclease 1 family [29], was found to inhibit HCC progression by inhibiting glycolysis in HCC cells and thereby facilitating the TCA cycle involving in the PTPN2-HK2 and CEBPβ-p53-PFK1 pathways [30]. In this study, elevated *CPS11* were associated with lower risk scores, however, the regulatory mechanisms of *CPS11* involved in advanced HCC remains unclear. As for the genes that exhibit a positive correlation with the risk score, it has been observed that *SPP1*, which is a glycoprotein that undergoes phosphorylation and secretion and possesses multiple functions, has been linked to unfavorable prognosis in numerous cancer types [31]. *G6PD*

is characterized as rate limitation and key enzyme of the pentose phosphate pathway. Its aberrant activation induces the enhancement of cell proliferation and adaptative capacity of many cancers [32]. This is achieved by maintaining intracellular redox homeostasis and promoting tumor growth [33]. *CDCA8* is a constituent of the chromosomal guest complex (CPC) and encodes a Borealin/Dasra B protein [34]. *CDCA8* plays a crucial function in liver tumorigenesis by regulating mitotic-related functions [35]. Patients who exhibit elevated levels of *CDCA8* are more likely to experience a negative prognosis [34]. Overall, our research outcomes align with prior domestic and international studies, suggesting that the effectiveness of our signature in prognosticating HCC patients remains strong.

Major breakthrough has been achieved in managing the late-stage HCC patients through the utilization of chemotherapy, TACE, and targeted therapy. Gemcitabine is an antimetabolic antitumor agent [36]. Cisplatin is a cell cycle non-specific agent [37]. Sorafenib is a potent inhibitor of multiple kinases, effectively suppressing tumor cell growth by targeting Raf-1, B-Raf, and other kinases involved in the Ras/Raf/MEK/ERK signaling pathway [38]. All these treatments have achieved significant efficacy in some HCC patients. However, the emergence of drug resistance has limited its application [39]. Therefore, exploring effective methods for screening sensitive populations would be beneficial for precision treatment. Based on the risk score, we conducted a sensitivity analysis on chemotherapy medications for patients. The findings indicated that cisplatin and gemcitabine exhibited higher efficacy in patients with lower risk scores. Besides, the prognostic signature was also predictive of the response of sorafenib and TACE. Patients who have high CRGs risk scores were discovered to be better candidates for sorafenib treatment, whereas those with low CRGs risk scores were deemed more appropriate for TACE therapy These discoveries were expected to provide innovative facets on the management of patients with HCC.

All 8 CRGs are closely related to metabolism, which is also confirmed by functional enrichment analysis. The most recent study indicates a strong correlation between HCC and lipid metabolism, whereby the liver-specific removal of *SETD2* results in decreased expression of *H3K36me3* and genes responsible for cholesterol efflux. Consequently, this leads to an accumulation of lipids, ultimately promoting the development of HCC [40]. According to the study conducted by Zhao et al., there was a suppression observed in the amino acid metabolic pathways among individuals diagnosed with HCC [41]. We had similar result that amino acid metabolism and lipid metabolism were negatively correlated to risk scores. Interestingly, we also noticed that most metabolic pathways had negative correlation to prognostic score, while glycan biosynthesis and metabolism showed positive correlation with risk score. Previous studies have stated that the peptide N-acetylgalactosaminyltransferases (GALNTs) in the Golgi apparatus can initiate mucin-type o-glycosylation [42], then confer a malignant phenotype on HCC cells by modifying EGFR O-glycosylation and activating the PI3K/AKT signaling pathway; this process is involved in the pathogenesis of HBV-associated HCC. Further study also indicated that down-regulation of *GALNTs* is related to poor prognosis of HCC patients [43]. Similar to previous studies, our results regarding other metabolic pathways also showed positive correlations to risk score. Moreover, the regulation of UBE2T on k63-ubiquitination and Akt phosphorylation has been found to initiate nuclear translocation of β-linked proteins, thus upregulating de novo pyrimidine synthesis-related enzymes and increasing pyrimidine metabolites to promote HCC development [44]. *DPP4i* inhibits Nash-related HCC progression by inhibiting the p62/Keap1/Nrf2 pathway and downregulating the pentose phosphate pathway [45]. Elucidating the association between the signature and metabolic pathways in HCC is significant to elaborate the molecular changes that may lead to the progression and metastasis of HCC. Thus, these result might contribute to explore potential anti-cancer regimes by altering the status of these metabolic pathways in the future.

In summary, the involvement of cuproptosis regulators is a crucial determination of the survival in HCC patients. Those with an elevated risk score for CRGs exhibited a poorer prognosis, reduced responsiveness to cisplatin and gemcitabine treatments, as well as distinct reactions to sorafenib and TACE. Therefore, we speculate that this regulation is achieved by altering the metabolism status. In this study, the molecular regulation pattern of CRGs was explored among HCC patients, providing a reference for developing new therapeutic targets and optimizing treatment strategies for advanced HCC.

Funding

This research did not receive any specific grant from funding agencies in the public, commercial, or not-for-profit sectors.

Data availability

All data analyzed in this study were available from publicly online databases TCGA (https://portal.gdc.cancer.gov/), GEO (https://www.ncbi.nlm.nih.gov/geo/) and PCAWG (https://dcc.icgc.org/pcawg/). Information about each data set was presented in the manuscript.

Ethics declarations

Review and/or approval by an ethics committee was not needed for this study because this study does not deal with ethics, so does the informed consent.

CRediT authorship contribution statement

Xin Qu: Formal analysis, Investigation. **Ling-cui Meng:** Formal analysis, Investigation. **Xi Lu:** Data curation, Investigation. **Xian Chen:** Data curation. **Yong Li:** Data curation. **Rui Zhou:** Conceptualization, Resources. **Yan-juan Zhu:** Methodology. **Yi-chang Luo:** Methodology. **Jin-tao Huang:** Writing – original draft, Writing – review & editing. **Xiao-liang Shi:** Writing – original draft, Writing –

review & editing. **Hai-Bo Zhang:** Conceptualization, Resources.

Declaration of competing interest

The authors declare that they have no known competing financial interests or personal relationships that could have appeared to influence the work reported in this paper.

Appendix A. Supplementary data

Supplementary data to this article can be found online at https://doi.org/10.1016/j.heliyon.2023.e23686.

References

[1] H. Sung, Id Orcid, J. Ferlay, et al., Global Cancer Statistics, 2020: GLOBOCAN estimates of Incidence and mortality worldwide for 36 cancers in 185 Countries, Ca - Cancer J. Clin. 71 (3) (2021) 209–249.
[2] X. Jiang, Id Orcid, B.R. Stockwell, et al., - Ferroptosis: mechanisms, biology and role in disease, Nat. Rev. Mol. Cell Biol. 22 (4) (2021) 266–282.
[3] P. Tsvetkov, Id Orcid, S. Coy, et al., Copper induces cell death by targeting lipoylated TCA cycle proteins, Science 375 (6586) (2022) 1254–1261.
[4] Z. Zhang, Y. Ma, X. Guo, et al., FDX1 can impact the prognosis and mediate the metabolism of lung adenocarcinoma, Front. Pharmacol. 12 (749134) (2021), 749134.
[5] K. Lossow, M. Schwarz, A.P. Kipp, Are trace element concentrations suitable biomarkers for the diagnosis of cancer? Redox Biol. 42 (2021), 101900.
[6] E. Urso, M. Maffia, - behind the link between copper and angiogenesis: established mechanisms and an overview on the role of vascular copper transport systems, J. Vasc. Res. 52 (3) (2015) 172–196.
[7] Y. Feng, J.W. Zeng, Q. Ma, et al., - Serum copper and zinc levels in breast cancer: a meta-analysis, J. Trace Elem. Med. Biol. 62 (126629) (2020).
[8] M. Zhang, M. Shi, Y. Zhao, Association between serum copper levels and cervical cancer risk: a meta-analysis, Biosci. Rep. 38 (4) (2018).
[9] R. Zhou, Id Orcid, H.C. Ma, et al., Dissecting the ferroptosis-related prognostic biomarker and immune microenvironment of driver gene-negative lung cancer, Exp. Biol. Med. 247 (16) (2022) 1447–1465.
[10] A. Mora, IM. - iRefR. Donaldson, An R package to manipulate the iRefIndex consolidated protein interaction database, BMC Bioinf. 12 (455) (2011) 1471–2105.
[11] M.D. Wilkerson, D.N. Hayes, ConsensusClusterPlus, A class discovery tool with confidence assessments and item tracking, Bioinformatics 26 (12) (2010) 1572–1573.
[12] G. Li, W. Xu, L. Zhang, et al., Development and validation of a CIMP-associated prognostic model for hepatocellular carcinoma, EBioMedicine 47 (2019) 128–141.
[13] J. Rao, X. Wu, X. Zhou, et al., - Development of a prognostic model for hepatocellular carcinoma using genes involved in aerobic respiration, Aging 13 (9) (2021) 13318–13332.
[14] X. Dai, W. Jiang, L. Ma, et al., A metabolism-related gene signature for predicting the prognosis and therapeutic responses in patients with hepatocellular carcinoma, Ann. Transl. Med. 9 (6) (2021) 21–927.
[15] Y. Tang, C. Guo, C. Chen, et al., Characterization of cellular senescence patterns predicts the prognosis and therapeutic response of hepatocellular carcinoma, Front. Mol. Biosci. 9 (1100285) (2022), 1100285.
[16] Y. Tang, C. Guo, Z. Yang, et al., Identification of a tumor immunological phenotype-related gene signature for predicting prognosis, immunotherapy efficacy, and drug candidates in hepatocellular carcinoma, Front. Immunol. 13 (862527) (2022).
[17] Y. Zhang, Y. Tang, C. Guo, et al., Integrative analysis identifies key mRNA biomarkers for diagnosis, prognosis, and therapeutic targets of HCV-associated hepatocellular carcinoma, Aging 13 (9) (2021) 12865–12895.
[18] J.M. Llovet, S. Ricci, V. Mazzaferro, et al., Sorafenib in advanced hepatocellular carcinoma, N. Engl. J. Med. 359 (4) (2008) 378–390.
[19] G.L. Su, O. Altayar, R. O' Shea, et al., AGA clinical practice guideline on systemic therapy for hepatocellular carcinoma, Gastroenterology 162 (3) (2022) 920–934.
[20] J.D. Yang, P. Hainaut, G.J. Gores, et al., A global view of hepatocellular carcinoma: trends, risk, prevention and management, Nat. Rev. Gastroenterol. Hepatol. 16 (10) (2019) 589–604.
[21] R.L. Siegel, Id Orcid, K.D. Miller, et al., - Cancer statistics, 2020, Ca - Cancer J. Clin. 70 (1) (2020) 7–30.
[22] T. Atakul, S.O. Altinkaya, Id Orcid, et al., - serum copper and zinc levels in patients with endometrial cancer, Biol. Trace Elem. Res. 195 (1) (2020) 46–54.
[23] J.O. Miners, D.J. Birkett, Cytochrome P4502C9: an enzyme of major importance in human drug metabolism, Br. J. Clin. Pharmacol. 45 (6) (1998) 525–538.
[24] D. Yu, B. Green, A. Marrone, et al., Suppression of CYP2C9 by microRNA hsa-miR-128-3p in human liver cells and association with hepatocellular carcinoma, Sci. Rep. 5 (8534) (2015).
[25] M. Seimiya, T. Tomonaga, K. Matsushita, et al., Identification of novel immunohistochemical tumor markers for primary hepatocellular carcinoma; clathrin heavy chain and formiminotransferase cyclodeaminase, Hepatology 48 (2) (2008) 519–530.
[26] N. Kanarek, H.R. Keys, J.R. Cantor, et al., - Histidine catabolism is a major determinant of methotrexate sensitivity, Nature 559 (7715) (2018) 632–636.
[27] J. Chen, Z. Chen, Z. Huang, et al., - formiminotransferase cyclodeaminase suppresses hepatocellular carcinoma by modulating cell apoptosis, DNA damage, and phosphatidylinositol 3-kinases (PI3K)/Akt signaling pathway, Med. Sci. Mon. Int. Med. J. Exp. Clin. Res. 25 (2019) 4474–4484.
[28] Z. Wang, X. Chen, Z. Jiang, SLC17A2 expression correlates with prognosis and immune infiltrates in hepatocellular carcinoma, Comb. Chem. High Throughput Screen. 25 (12) (2022) 2001–2015.
[29] P.A. Keyel, Dnases in health and disease, Dev. Biol. 429 (1) (2017) 1–11.
[30] Y. Xiao, K. Yang, P. Liu, et al., - deoxyribonuclease 1-like 3 inhibits hepatocellular carcinoma progression by inducing apoptosis and reprogramming glucose metabolism, Int. J. Biol. Sci. 18 (1) (2022) 82–95.
[31] L. Shi, X. Wang, Role of osteopontin in lung cancer evolution and heterogeneity, Semin. Cell Dev. Biol. 64 (2017) 40–47.
[32] H.C. Yang, Y.H. Wu, W.C. Yen, et al., The redox role of G6PD in cell growth, cell death, and cancer, Cells 8 (9) (2019).
[33] T. Cai, Y. Kuang, C. Zhang, et al., Glucose-6-phosphate dehydrogenase and NADPH oxidase 4 control STAT3 activity in melanoma cells through a pathway involving reactive oxygen species, c-SRC and SHP2, Am. J. Cancer Res. 5 (5) (2015) 1610–1620.
[34] Y. Shuai, E. Fan, Q. Zhong, et al., CDCA8 as an independent predictor for a poor prognosis in liver cancer, Cancer Cell Int. 21 (1) (2021) 21–1850.
[35] L. Li, D. Li, F. Tian, , et al.L. Li, D. Li, F. Tian, J. Cen, X. Chen, Y. Ji, L. Hui, Hepatic loss of Borealin impairs postnatal liver development, regeneration, and hepatocarcinogenesis, J. Biol. Chem. 291 (40) (2016) 21137–21147 [J].J Biol Chem, 2016, 291(40): 21137-21147.
[36] F. Attia, S. Fathy, M. Anani, et al., Human equilibrative nucleoside transporter-1 and deoxycytidine kinase can predict gemcitabine effectiveness in Egyptian patients with Hepatocellular carcinoma, J. Clin. Lab. Anal. 34 (11) (2020).
[37] D. Wang, S.J. Lippard, - Cellular processing of platinum anticancer drugs, Nat. Rev. Drug Discov. 4 (4) (2005) 307–320.
[38] A. Gauthier, M. Ho, Role of sorafenib in the treatment of advanced hepatocellular carcinoma: an update, Hepatol. Res. 43 (2) (2013) 147–154.

[39] Z. Zhang, Id Orcid, C. Shen, et al., The natural medicinal fungus Huaier promotes the anti-hepatoma efficacy of sorafenib through the mammalian target of rapamycin-mediated autophagic cell death, Med. Oncol. 39 (12) (2022) 22–1797.
[40] X.J. Li, Q.L. Li, L.G. Ju, et al., Deficiency of histone methyltransferase SET domain-containing 2 in liver leads to abnormal lipid metabolism and HCC, Hepatology 73 (5) (2021) 1797–1815.
[41] Y. Zhao, J. Zhang, S. Wang, et al., Identification and validation of a nine-gene amino acid metabolism-related risk signature in HCC, Front. Cell Dev. Biol. 9 (731790) (2021), 731790.
[42] K.G. Ten Hagen, T.A. Fritz, L.A. Tabak, All in the family: the UDP-GalNAc:polypeptide N-acetylgalactosaminyltransferases, Glycobiology 13 (1) (2003) 1.
[43] Q. Wu, H.O. Liu, Y.D. Liu, et al., Decreased expression of hepatocyte nuclear factor 4α (Hnf4α)/microRNA-122 (miR-122) axis in hepatitis B virus-associated hepatocellular carcinoma enhances potential oncogenic GALNT10 protein activity, J. Biol. Chem. 290 (2) (2015) 1170–1185.
[44] Z. Zhu, Id Orcid, C. Cao, et al., UBE2T-mediated Akt ubiquitination and Akt/β-catenin activation promotes hepatocellular carcinoma development by increasing pyrimidine metabolism, Cell Death Dis. 13 (2) (2022) 22–4596.
[45] T. Kawaguchi, D. Nakano, H. Koga, et al., Effects of a DPP4 inhibitor on progression of NASH-related HCC and the p62/keap1/nrf2-pentose phosphate pathway in a mouse model, Liver Cancer 8 (5) (2019) 359–372.